Herbivory and Temperature Mediate Coral Reef Halo Dynamics

Anne A. Innes-Gold,[1,*] Lisa C. McManus,[1] Emily Lester,[2] Theresa W. Ong,[3] Aimee Cook McNab,[1] Sophia A. Rahnke,[1] Joshua Brett Pablo,[1] Ann Tokoyoda,[1] Dava Watson,[1] and Elizabeth M. P. Madin[1]

1. Hawai'i Institute of Marine Biology, University of Hawai'i at Mānoa School of Ocean and Earth Science and Technology, Kāne'ohe, Hawai'i 96744; 2. School of Geosciences, University of Sydney, Sydney, Australia; 3. Department of Environmental Studies, Graduate Program in Ecology, Evolution, Environment and Society, Dartmouth College, Hanover, New Hampshire 03755

Submitted November 1, 2024; Accepted June 6, 2025; Electronically published November 4, 2025

Online enhancements: supplemental PDF.

ABSTRACT: Reef halos are rings of sand, barren of vegetation, encircling reefs. However, the extent to which various biotic (e.g., herbivory) and abiotic (e.g., temperature, nutrients) factors drive changes in halo prevalence and size remains unclear. The objective of this study was to explore the effects of herbivore biomass, primary productivity, temperature, and nutrients on reef halo presence and width. First, we conducted a field study using artificial reef structures and their surrounding halos, finding that halos were more likely to be observed with high herbivorous fish biomass and that halos were larger under high temperatures. There was a distinct interaction between herbivorous fish biomass and temperature, where at high fish biomass, halos were more likely to be observed under low temperatures. Second, we incorporated environmental drivers into a consumer-resource model of halo dynamics. Certain formulations of temperature- and nutrient-dependent vegetation growth caused halo width and fish density to change from a fixed to an oscillating system, supporting the idea that environmental drivers can cause temporal fluctuations in halo width. Our unique combination of field-based and mechanistic modeling approaches has enhanced our understanding of the role of environmental drivers in grazing patterns, which will be particularly important as climate change causes shifts in marine systems worldwide.

Keywords: consumer-resource, coral reef, herbivory, predation risk, reef halo, spatial patterns, species interactions.

Introduction

Reef halos are rings of sand, barren of vegetation, encircling coral reefs. These bands typically extend from meters to tens of meters in width, surrounding patch reefs that can be observed in satellite imagery (Madin et al. 2022). The primary hypothesis for the mechanism behind reef halos relates to spatially constrained herbivory by fish and invertebrates due to predation risk (i.e., landscape of fear), termed the "grazing hypothesis" (Ogden et al. 1973; Valentine et al. 2007). Patch reefs offer refuge from predation risk by providing shelter to smaller herbivorous fish and invertebrates (Almany 2004). Thus, herbivores tend to focus their grazing in the vicinity of the patch reef, resulting in the absence of benthic vegetation directly surrounding the patch reef (Madin et al. 2010). There are other mechanisms that may contribute to halo formation and/or maintenance; however, the evidence of their impact is less conclusive. Some of these potential drivers include bioturbation (Alevizon 2002; Steiner and Willette 2014; Madin et al. 2019*b*), nutrient toxicity (Alevizon 2002), sediment deposition (Garrett et al. 1971), and water movement (Steiner and Willette 2014).

While halos can persist for more than 50 years, halo width can be highly dynamic over space and time (Madin et al. 2022). In general, the width of a halo at a given patch reef is known to vary with patch reef size (Madin et al. 2019*a*) and has been shown in at least one system to also be driven by herbivore abundance (DiFiore et al. 2019). However, individual halos can change in size over relatively short (month-to-month) timescales (Madin et al. 2022). Such fluctuations in halo size have been observed around the globe, including in Australia, Guam, United States, Fiji, and Egypt (Madin et al. 2022). These changes in size have led researchers to believe that mechanisms other than those previously identified may play a role in halo formation. There is evidence that halo "disappearances" from satellite imagery are due to shifts in the composition of the algal meadows that form the background for halos rather than the breakdown of halo-forming mechanisms (Madin et al. 2022).

* Corresponding author; email: ainnesgo@hawaii.edu.

ORCIDs: Innes-Gold, https://orcid.org/0000-0003-0949-6826; McManus, https://orcid.org/0000-0002-9367-6872; Lester, https://orcid.org/0000-0003-2207-5225; Ong, https://orcid.org/0000-0002-7291-5205; McNab, https://orcid.org/0000-0002-3109-1385; Rahnke, https://orcid.org/0009-0006-7843-5495; Madin, https://orcid.org/0000-0002-2391-2542.

American Naturalist, volume 206, number 6, December 2025. Published by The University of Chicago Press for The American Society of Naturalists. https://doi.org/10.1086/738015

Outside of the previously mentioned hypothesized mechanisms of halo dynamics, water temperature and nutrient levels are strong drivers of vegetation growth (Lee et al. 2007; Singh and Singh 2015) and fish grazing rates (Ferreira et al. 1998; Alevizon 2002; Campbell et al. 2018; Goss et al. 2018) and thus may affect the observed fluctuations in halo width. Reef halo width was found to be correlated with sea surface temperature (SST) in one study (higher SST led to larger halos), although patch reef size was a confounding variable in this relationship because warmer areas had larger patch reefs in the area studied (Madin et al. 2019*a*). It remains unclear how these abiotic factors might interact with biotic drivers, such as herbivory and primary productivity, to influence the landscape of fear dynamics. Additionally, the potential for interactions among these biotic and abiotic factors, as well as the various scales of measurements used across different studies, may be adding to the equivocal results.

The objective of this study was to explore the effects of herbivore biomass, primary productivity, temperature, and nutrients on halo presence, width, and vegetation cover. First, we conducted a field study using artificial reef structures in Kāneʻohe Bay, Oʻahu, Hawaiʻi (fig. 1), and their surrounding halos to assess correlations between halo presence, width, and vegetation cover with background vegetation, fish communities, SST, and nutrient levels. Given that Kāneʻohe Bay is an estuary with strong seasonal dynamics, including fluctuating nutrient inputs (Drupp et al. 2011), we expected that temperature and nutrient availability (e.g., nitrogen and phosphorus), as well as herbivorous fish biomass, would affect vegetation.

Second, we explored causal effects of environmental drivers (SST, nutrients) on halo width by incorporating said drivers into a consumer-resource model of halo dynamics. The first part of our study reveals in situ correlations between halos and environmental drivers, while the second part explores the potential for temperature- and nutrient-dependent vegetation growth to mediate halo dynamics within a modeling framework. Uncertainty regarding the relative contribution of various mechanisms to halo formation persists, partly because of a lack of experimental studies and because previous models have not adequately integrated both biotic and abiotic factors. Our study's combination of a field experiment with a mechanistic modeling approach provides a unique perspective to uncover drivers of halo dynamics.

Methods

In Situ Study: Kāneʻohe Bay, Oʻahu, Hawaiʻi

Reef Construction. In February 2022 we built three artificial reef structures on areas of mixed seagrass (*Halophila* sp.) and algae in Kāneʻohe Bay, Oʻahu, Hawaiʻi (fig. 1). The structures were spaced at least 30 m from each other, that is, far enough to discourage movement of herbivores between reef structures (Turgeon et al. 2010) but close enough to reduce variation of large-scale environmental factors. After constructing the reefs, we had an adjustment period of ~6 months (Alevizon and Gorham 1989; Clark and Edwards 1994), which allowed ample time for the reef structures to be colonized by relatively stable fish communities and for apparent halos to be visible. Each artificial

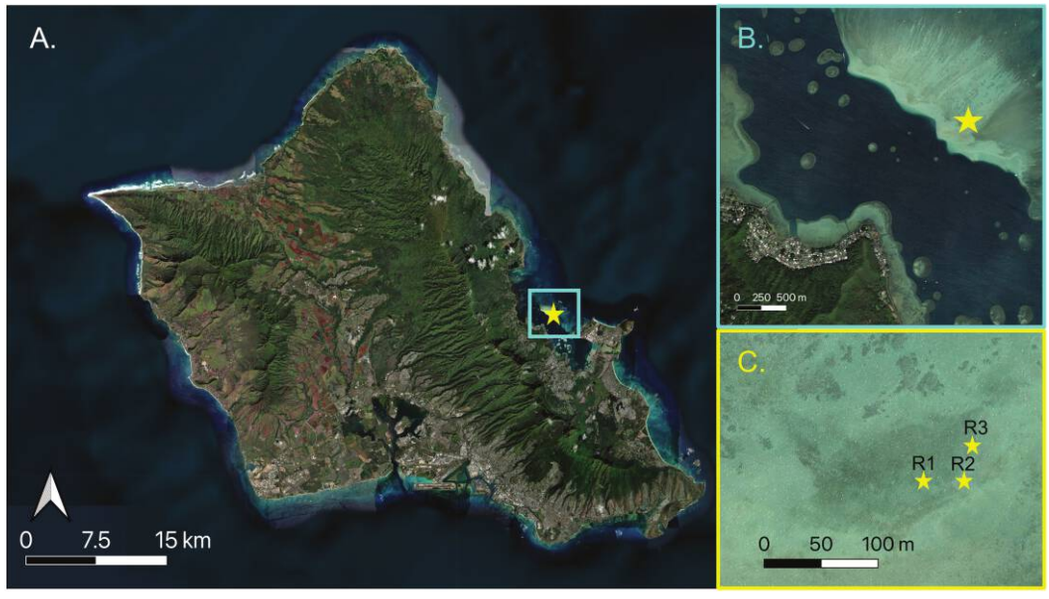

Figure 1: Map of our study area across scales. *A*, Oʻahu, Hawaiʻi. *B*, Kāneʻohe Bay. *C*, Artificial reef locations within Kāneʻohe Bay.

reef was constructed of eight cinder blocks, with a bottom layer of four blocks, an upper layer of three blocks, and one block in the top center (fig. 2*A*). The cinder blocks were zip-tied together to form one unit but were not glued to the substrate. There is minimal water movement in the study area, and they stayed in this configuration for the entire study duration. Once a month, from August 2022 to December 2023, we took water samples for nutrient analysis and surveyed vegetation cover and fish communities.

Sea Surface Temperature. SST was recorded continuously using HOBO pendant temperature loggers attached to the central cinder block at each artificial reef. The logger recorded the temperature every 6 h for the entire duration of the study. Our SST measures were the rolling averages of the 14 days before the vegetation surveys were conducted. SST data for the first 2 months (August and September 2022) came from the nearby National Oceanic and Atmospheric Administration buoy (https://www.ndbc.noaa.gov/; station 51207, which is located ~5 km northeast of the artificial reefs at 21°28′39″N, 157°45′7″W) because of logger loss.

Nutrients. Water samples were taken monthly, at the same time that the fish surveys and vegetation transects were conducted. One water sample was taken per reef. The samples were analyzed for phosphate (μmol/L) and nitrate + nitrite (NN; μmol/L). Water samples were analyzed by the University of Hawai'i at Mānoa SOEST Laboratory for Analytical Biogeochemistry (see the supplemental PDF [available online] for a full description of analytic procedures).

Herbivore and Nonherbivore Biomass. Fish community surveys were conducted monthly at the same time as nutrient sampling and vegetation transects. Surveys were conducted by the same observer each time who would sit ~3 m away from the reef to minimize disturbance and record all fish seen within 1 m of the reef for 3 min. After that time, the observer would move to the reef and attempt for another 2 min to record any fish that may not have been initially visible. This was repeated at each of the three artificial reefs. For each species, the abundance and approximate length of each individual was recorded and classified as an herbivore or nonherbivore (Froese and Pauly 2024). Abundances were converted to biomass using established species- or genus-specific length-weight equations (table S1; tables S1–S7 are available online). Biomass for herbivores and nonherbivores was separately summed to obtain herbivorous fish biomass and nonherbivorous fish biomass for each reef at each survey.

Mean Vegetation Cover. We recorded three 5-m-long video transects, spaced evenly around the reef, starting from each of the three top-layer cinder blocks of the artificial reef, positioned perpendicularly to the cinder block and going outward into the seagrass meadow. On each video transect, photos were taken continuously starting at the artificial reef. Each photo was imported into ImageJ (Schneider et al. 2012), where the scale was set based on a 10-cm measure on the transect, and then a virtual 20 × 20-cm quadrat was laid directly on the right side of the transect. Virtual quadrats were laid consecutively every 20 cm (e.g., a quadrat at 0–20, 20–40, and 40–60 cm; here termed "distance bins"). Then, 20 random points were generated

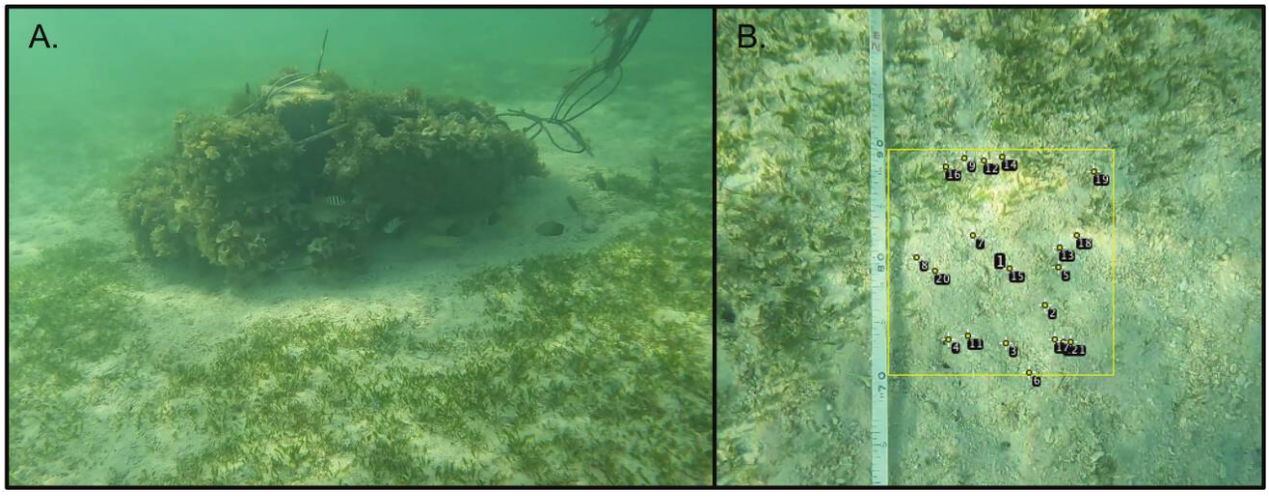

Figure 2: *A*, One of three artificial reefs constructed in a seagrass bed in December 2023 (pictured 22 months after deployment), showing the three 5-m transects taken at each reef and a visualization of the mean vegetation cover, halo vegetation cover, and halo width metrics. *B*, Virtual quadrat and random points generated to quantify halo vegetation cover and halo width.

inside each distance bin (fig. 2*B*) and classified as sand or vegetation. Percent vegetation cover was calculated for each distance bin as the number of vegetation points/total points (25 bins per transect). We then calculated the mean vegetation cover at a reef by averaging all bins for the three transects.

Halo Presence, Width, and Vegetation Cover. We calculated the halo width based on the number of bins that had percent vegetation cover below 1 SD from the mean. For example, we averaged the three 0–20-cm bins for a reef (one from each transect) to get an average for that distance bin as the average vegetation cover 0–20 cm from the reef. If this averaged bin had vegetation cover lower than 1 SD below the mean vegetation cover of that reef and the averaged bin at the next distance (20–40 cm) away from the reef had vegetation cover within 1 SD of the mean, then the halo width was recorded as 20 cm. If none of the averaged bins had vegetation cover greater than 1 SD below the mean, we determined that a halo was not present. If a halo was present, it was characterized by halo width (distance from structure to halo boundary [cm]) and halo vegetation cover (average percent vegetation cover inside the boundaries of the halo). Halo width provides information on how the boundaries of the halo are fluctuating over time, while halo vegetation cover provides a metric of how distinct the halo is from the surrounding vegetation (e.g., lower halo vegetation cover means a more distinct halo; fig. 2).

Statistical Analysis. All analyses were conducted in R (ver. 4.4.0; R Core Team 2024). We used generalized linear mixed effects models (GLMMs) to account for random and fixed factors. In all models, reef number and month were specified as random effects. For simplicity and ease of interpretation, GLMMs were the default method, and generalized additive mixed models (GAMMs) were used when the assumptions of normality did not hold (hypotheses 3 and 4). There was no evidence of collinearity between predictor variables (correlation coefficients <0.7; Akoglu 2018; fig. S1; figs. S1–S7 are available online).

We established the following four hypotheses and corresponding models to guide our analysis.

Hypothesis 1. Mean vegetation cover may be influenced by temperature, nutrient availability (NN, phosphate), herbivorous fish biomass, and the interaction between herbivorous fish and temperature (model: mean vegetation cover ~ SST + NN + phosphate + herbivorous fish biomass + SST × herbivorous fish [GLMM, binomial family used for proportion data, package lme4; Bates et al. 2015]). This interaction was included because of the potential for herbivorous fish metabolism, and thus grazing rates, to increase as temperatures fluctuate (Volkoff and Rønnestad 2020).

Hypothesis 2. Halo presence may be influenced by temperature, primary productivity (mean vegetation cover), herbivorous fish biomass, nonherbivorous fish biomass, and the interaction between herbivorous fish and temperature (model: halo presence ~ mean vegetation cover + SST + herbivorous fish biomass + nonherbivorous fish biomass + SST × herbivorous fish [GLMM, binomial family, package lme4; Bates et al. 2015]).

Hypothesis 3. Halo width may be influenced by temperature, primary productivity (mean vegetation cover), herbivorous fish biomass, nonherbivorous fish biomass, and the interaction between herbivorous fish and temperature (model: halo width ~ mean vegetation cover + SST + herbivorous fish biomass + nonherbivorous fish biomass + SST × herbivorous fish [GAMM, Gaussian family, package mgcv; Wood 2017]).

Hypothesis 4. Halo vegetation cover may be influenced by temperature, primary productivity (mean vegetation cover), herbivorous fish biomass, nonherbivorous fish biomass, and the interaction between herbivorous fish and temperature (model: halo vegetation cover ~ mean vegetation cover + SST + herbivorous fish biomass + nonherbivorous fish biomass + SST × herbivorous fish [GAMM, binomial family, package mgcv; Wood 2017]).

Theoretical Study: Consumer-Resource Model

We adapted an existing consumer-resource model of halo dynamics (Ong et al. 2025) to mechanistically understand shifts in halo patterns across a range of abiotic conditions. Ong et al. (2025) developed a spatially implicit consumer-resource model that incorporated how predation risk and spatial distribution of reefs limits vegetation growth. Their model described change in vegetation and herbivore density as

$$\frac{dA}{dt} = \gamma A\left(1 - \frac{A}{A_0 e^{-R((A_0 - A)/r_c)}}\right) - \frac{gAH}{1 + gsA}, \quad (1)$$

$$\frac{dH}{dt} = \frac{rAH}{1 + gsA}\left(1 - \frac{H}{(1 - A_0)k}\right) - mH, \quad (2)$$

where A represents vegetation density, γ is the vegetation growth rate, A_0 is the maximum vegetation cover, R is a measure of the spatial distribution of coral reefs, r_c is the radius of the central coral colonies, g is the grazing rate, s is the handling time of herbivores, r is the growth rate of herbivores, k is the carrying capacity of herbivores, and m is the herbivore mortality rate. These equations are derived from a geometric model (eqq. [S1]–[S4]), which provides a baseline expectation for how the landscape of fear hypothesis should limit vegetation cover given the spatial distribution

of shelter patches and a set distance limit for grazers. Thus, vegetation cover across a range of halo sizes (calculated as $A_0 - A$) is approximated with a nonlinear decreasing function. Although herbivores in this model are mean field, the growth and decline of vegetation cover and herbivores are constrained by the spatial distribution of the coral patches (R; Ong et al. 2025).

We characterized the spatial distribution of reefs with Clark-Evans R, which is calculated by comparing the observed mean distance between the nearest neighbor points with the expected mean distance from a random distribution. In general, $R < 1$ indicates clustering, while $R > 1$ indicates a dispersed pattern (Clark and Evans 1954). The landscape of fear constraints are embedded through the R term, where a clustered reef has less total grazing area available than a dispersed reef with the same coral density (fig. S2; Ong et al. 2025). In a dispersed reef system with more halos, vegetation becomes more limited because herbivores can occupy more space, leading to slightly stronger density dependence on vegetation growth (fig. S3).

Because the purpose of this analysis was to characterize temperature- and nutrient-driven changes in halo dynamics from a stable state, nearly all parameter values were arbitrary and held consistent from Ong et al. (2025); these values are presented in the captions for model results figures. We tested two versions of spatial distribution of reefs (Clark-Evans R, $R = 0.13$ and $R = 1.28$). These two values were based on our field site and calculated using the spatstat package in R (Baddeley et al. 2015). The first R value, 0.13, was calculated using a large boundary around the locations of our artificial reefs, including the natural reef area surrounding them, representing a highly clustered reef scenario that large, roving herbivore species could cover during their foraging (e.g., Welsh and Bellwood 2012). The second R value, 1.28, was using a small boundary just around one artificial reef, representing a dispersed reef with lower clustering that herbivores with relatively high site fidelity could cover (e.g., Ferguson et al. 2013). In addition to approximating distinct herbivore community types, the two R parameters represented high and low reef clustering that corresponded to fixed and cyclic baseline models, respectively. The cyclic formulation corresponding to the high R value occurs because in the dispersed scenario, there are more limitations on vegetation growth, since more feeding boundaries/halos are present.

We tested three formulations of vegetation growth. First, we tested baseline vegetation growth (γ_B): γ held constant at 0.8, the value used in Ong et al. (2025). Second, we tested temperature-dependent vegetation growth: we used a quadratic function to calculate a temperature-dependent vegetation growth rate at each daily time step. The maximum was 0.8, which occurred at the optimal temperature for growth. We tested low, medium, and high optimal temperatures to represent different seagrass and algae species (in range of Hillman et al. 1995; Ralph 1998; Lee et al. 2007; Collier et al. 2017; fig. 3*A*–3*C*). We used the temperature time series collected during the in situ study as input for the model (fig. 3*A*). Third, we tested nutrient-dependent vegetation growth: we used a logarithmic function to represent growth rate response to nutrient levels. We chose the shape of the function based on substantial previous work quantifying algal and other plant growth across increasing nutrient levels (Rier and Stevenson 2006; Dailer et al. 2012; Cott et al. 2018). We used the same maximum growth rate (0.8) and focused on nitrogen as the nutrient input because there is evidence that many marine systems, including Kāneʻohe Bay, are nitrogen limited (Ringuet and Mackenzie 2005; Bristow et al. 2017). Given that different vegetation species may have different optimal nitrogen conditions (Ingestad 1976; Monfet and Unc 2017), we tested a range of slope parameters to vary the nitrogen concentration where the maximum growth rate was reached (fig. 3*D*–3*F*). We used the total nitrogen time series collected in the in situ study as input for the model (fig. 3*D*).

We first solved the model for a burn-in period of 200 days to reach equilibrium using a constant value for vegetation growth rate, γ_B. We then incorporated temperature- or nutrient-dependent vegetation growth. For each formulation of vegetation growth, we tracked mean relative halo width across the seascape, calculated as $A_0 - A$, and herbivore density over time. Finally, we compared the mechanistic model and field study results by approximating the field sampling protocol within our temperature-dependent model system. To achieve this, we subsetted the model time series data for halo width and herbivore density at 30-day intervals, enabling us to discern patterns between these variables and compare them with the corresponding temperature values for each time step. We conducted this analysis for two optimal temperature scenarios for both the fixed model and the cyclic model. Because our field study temperature data fell between 24°C and 28°C, we chose a low optimal SST scenario of 24°C and a high optimal SST scenario of 28°C. We began the simulated sampling on day 0 (after the 200-day burn-in period) and ran an additional trial where we began sampling on day 15 (after the 200 day burn-in period) to assess whether the timing of sampling impacted observed patterns.

Results

In Situ Study

We observed fluctuations in halo presence and size over time at the three sites. Temporal trends in halo width, mean vegetation cover, halo vegetation cover, SST, fish biomass, NN, and phosphate are shown in figure S4. We

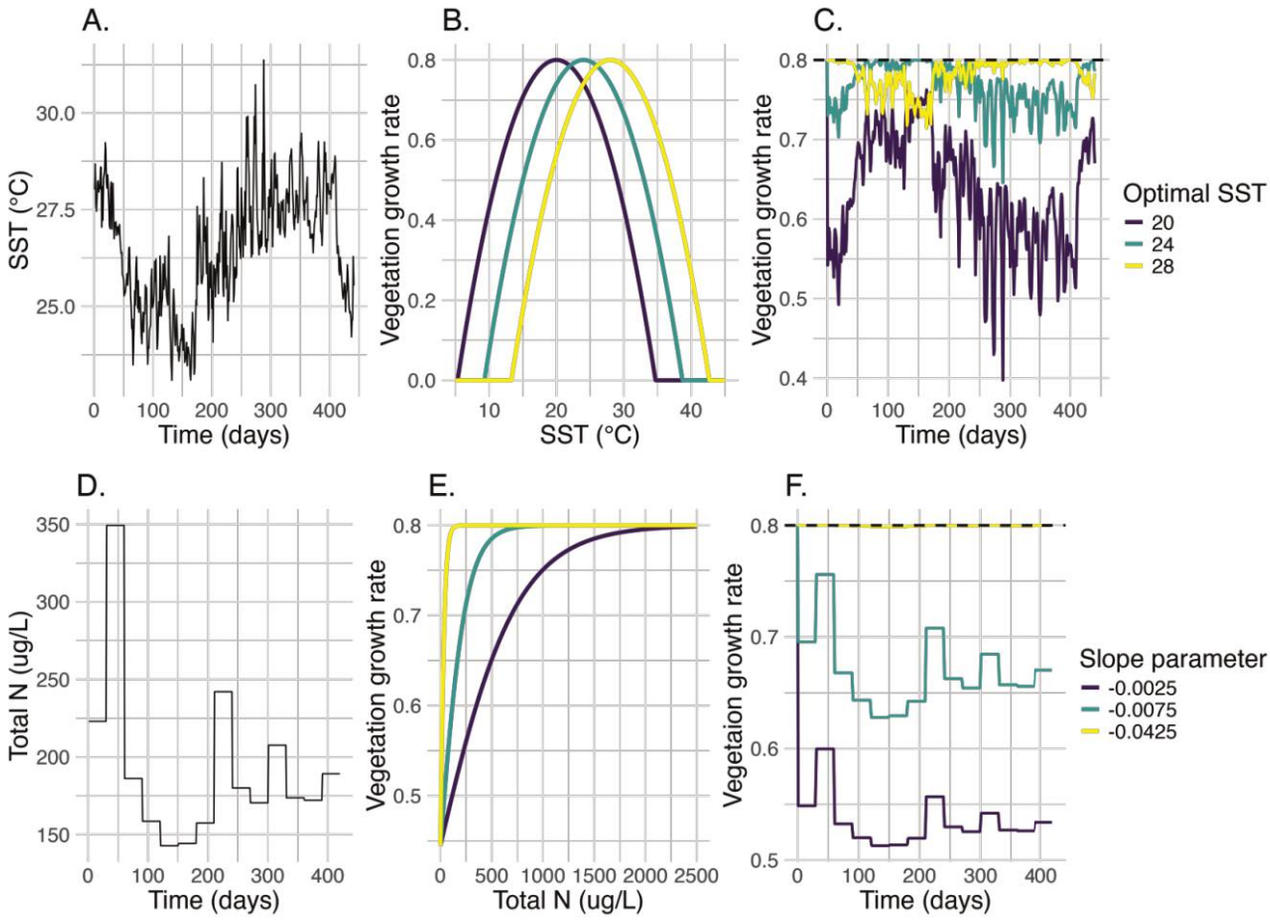

Figure 3: Vegetation growth rate response to sea surface temperature (SST; *A*–*C*) and nitrogen (*D*–*F*). *A*, SST time series collected from our field site and used as an input for calculating growth rate. *B*, Various formulations of temperature-dependent growth rate. *C*, Growth rates calculated at each time step based on the temperature. *D*, Nitrogen time series collected from our field site. *E*, Various formulations of nitrogen-dependent growth rate. *F*, Growth rates calculated at each time step based on nitrogen. Note that temperature was collected daily, while nitrogen was collected monthly and is assumed to remain constant throughout the month.

found that SST was a significant predictor of mean vegetation cover, with higher SST leading to lower mean vegetation cover (GLMM, $z = -2.4168$, $P = .016$; fig. 4*A*; table S2). We found that herbivorous fish biomass was significantly correlated with halo presence, with halos more likely to be present with higher herbivore biomass at a given point in time (GLMM, $z = 4.373$, $P < .001$; table S3). There was a significant effect of the interaction between SST and herbivorous fish biomass on halo presence ($z = -4.574$, $P < .001$). Halos were most likely to be observed at high herbivore biomass and low SST (fig. 4*B*). Halo presence was not significantly correlated with nonherbivore biomass ($z = -1.011$, $P = .312$).

For data where halos were observed, we explored drivers of halo width and halo vegetation density (percent vegetation cover inside the halo). Halo width was significantly correlated with SST (GAMM, $k = 6$, deviance explained = 64.5%, $F = 5.009$, $P = .023$; tables S4, S5), with higher SST leading to larger halos (fig. 4*C*). Halo vegetation cover was significantly correlated with mean vegetation cover (GAMM, $k = 3$, deviance explained = 80%, $\chi^2 = 40.157$, $P < .001$; fig. 4*D*; tables S6, S7), herbivore biomass ($t = -2.965$, $P = .003$), and the interaction between herbivore biomass and temperature ($t = 2.7853$, $P = .004$). Halo vegetation cover was likely to be lower (more sparse vegetation) under conditions of high herbivore biomass and low SST (fig. 4*E*). Halo width and vegetation cover were not correlated with nonherbivore biomass.

Theoretical Study: Consumer-Resource Model

To look at potential causal effects of temperature and nutrients on halo dynamics, we explored different formulations of

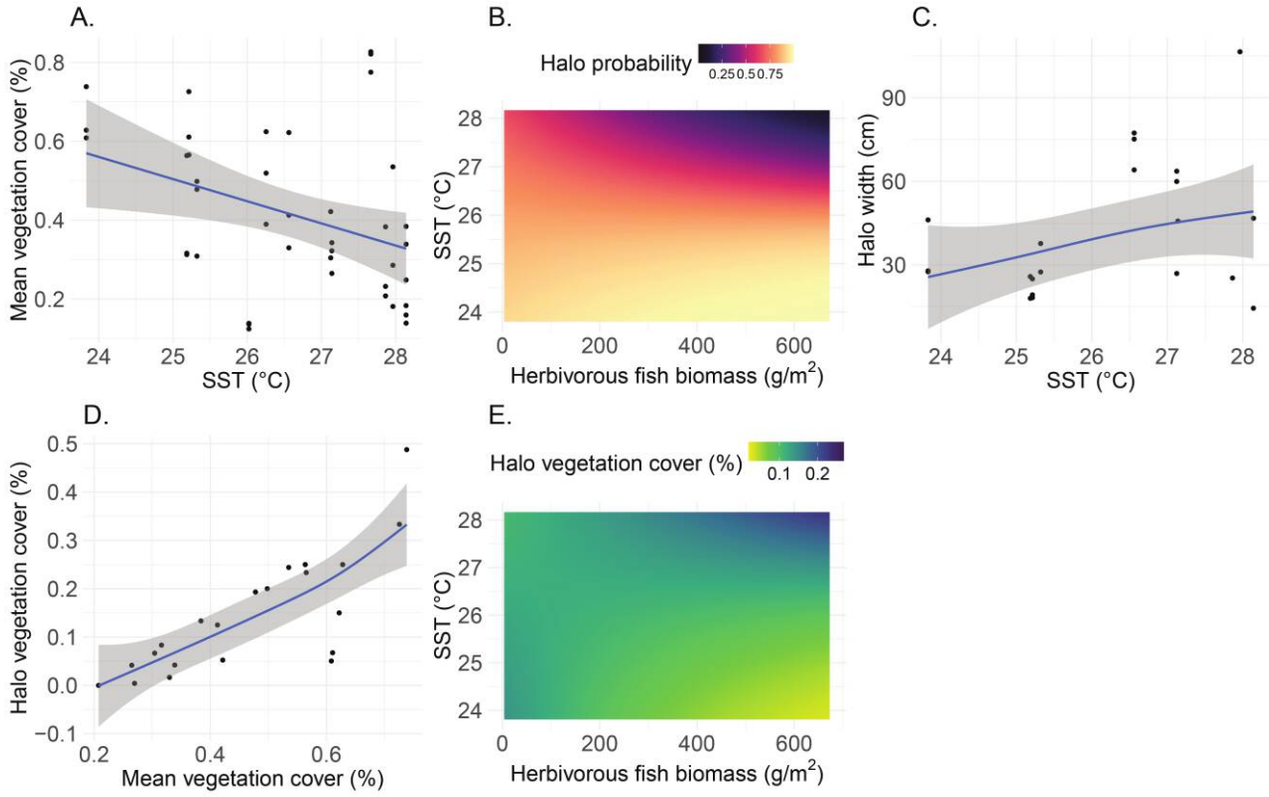

Figure 4: Significant correlations from our field study. *A*, Relationship between sea surface temperature (SST) and mean vegetation cover. *B*, Relationship between SST, herbivorous fish biomass, and halo probability. *C*, Relationship between SST and halo width. *D*, Relationship between mean vegetation cover and halo vegetation cover. *E*, Relationship between herbivorous fish biomass, SST, and halo vegetation cover.

temperature- and nutrient-dependent vegetation growth in a consumer-resource model. When growth rate was temperature dependent, the optimal temperature parameter played an important role in determining the behavior of the model (fig. 5). We first used a fixed baseline model, corresponding to a larger system boundary with high clustering ($R = 0.13$). Here, a low optimal temperature (20°C) caused both the halo width and the herbivore density trajectories to shift from a single fixed point to oscillations, representing a shift from halos with a fixed size to ones with dynamically variable widths over time (fig. 5*A*). Other optimal temperatures caused time-varying trajectories that increased halo width from the baseline by up to ~30% but led to no visible change to herbivore density. We then used a cyclic baseline model ($R = 1.28$), corresponding to a smaller system boundary that was more dispersed. Here, varying the optimal temperature caused changes in the timing and amplitude of the oscillations compared with the baseline model. However, all versions remained in stable oscillations (fig. 5*B*). For example, optimal temperatures at the lower end of our tested range led to generally earlier peaks in growth rate amplitude compared with the baseline model. The amplitude of halo width and herbivore density oscillations varied, likely because of the relationship between the SST time series and the set optimal temperature. For both halo width and herbivores, the amplitude of the lower optimal temperature cycles generally increased over time, while the amplitude of the higher optimal temperature cycles declined over time. The frequency of cycles remained consistent across optimal temperatures.

We saw similar results after implementing nutrient-dependent vegetation growth. When using a fixed baseline model, a less negative slope parameter (indicating a higher optimal nutrient concentration; e.g., −0.0025) caused the halo width and herbivore density to shift from a stable fixed point to oscillations (fig. S5*A*). When using a cyclic baseline model, varying the slope of the nutrient function led to changes in the timing and amplitude of the oscillations compared with the baseline model (fig. S5*B*).

To further understand the patterns and interactions we observed in our field study, we simulated sampling events in our temperature-dependent model trajectories to compare

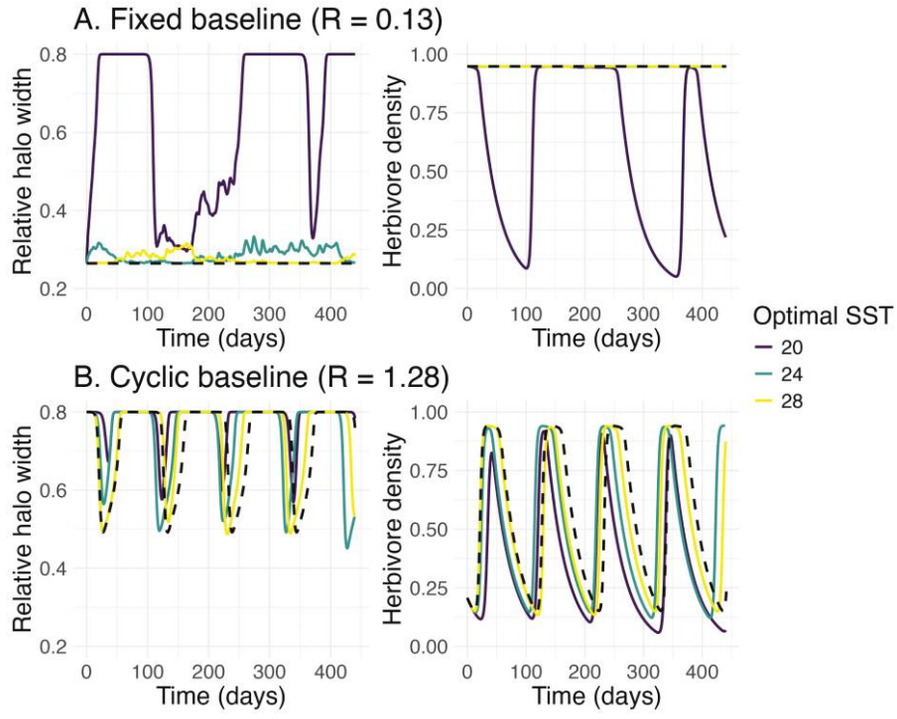

Figure 5: Results of the temperature-dependent consumer-resource model. The black dashed line represents the baseline model with no temperature dependencies. Parameters were $A_0 = 0.8$, $g = 2$, $k = 5$, $m = 0.03$, $r = 8$, $s = 6$, and $r_c = 2$. *A*, Fixed baseline version of the model corresponding to a larger system boundary and more clustered system ($R = 0.13$). For optimal sea surface temperatures (SSTs) above 20°C, there are no distinguishable changes to herbivore population trajectories. *B*, Cyclic baseline version of the model corresponding to a smaller system boundary and more dispersed system ($R = 1.28$).

patterns between SST, halo width, and herbivore density derived from the consumer-resource model. When using the fixed baseline model, there was a clear effect of temperature. Under the low optimal temperature scenario, halo width was smallest under high-herbivore and low-SST conditions (fig. 6*A*). Under the high optimal temperature scenario, halo width was smallest under high-herbivore and high-temperature scenarios (fig. 6*B*). This fixed baseline and low optimal temperature scenario most closely resembled our field observations, where halos were larger with high SST.

When using the cyclic baseline model, halo width was large at the majority of the simulated sampling events for both optimal temperature scenarios (fig. 6*C*, 6*D*). In these scenarios, smaller halos mainly occurred with high herbivore density, and there was no clear effect of temperature. We also simulated sampling every 30 days but beginning on day 15 to test whether sampling schedule impacted projected results. Overall, patterns remained largely consistent whether sampling began on day 0 (fig. 6) or day 15 (fig. S6). Finally, we tested the robustness of our model predictions to alternative parameter values. Specifically, for the dispersed scenario ($R = 1.28$), we might expect a lower maximum vegetation space (A_0), since more area is covered by reef, and a lower fish carrying capacity (k) because of the smaller domain. We ran the same simulated sampling analysis with $A_0 = 0.5$ and $k = 2$ and found that the overall qualitative patterns remained consistent (fig. S7).

Discussion

Our combination of field and modeling studies demonstrated that both biotic and abiotic factors can influence halo dynamics. Our field study showed that primary productivity, fish biomass, and SST were correlated with patterns of halo presence and width. Our mechanistic consumer-resource study showed that temperature and nutrient effects can cause the system to shift from fixed to cyclic halos that fluctuate in size over time. Additionally, through simulated sampling events in our consumer-resource model, we found that our field site most closely resembles the fixed, highly clustered reef scenario with a low optimal temperature. Our findings provide further

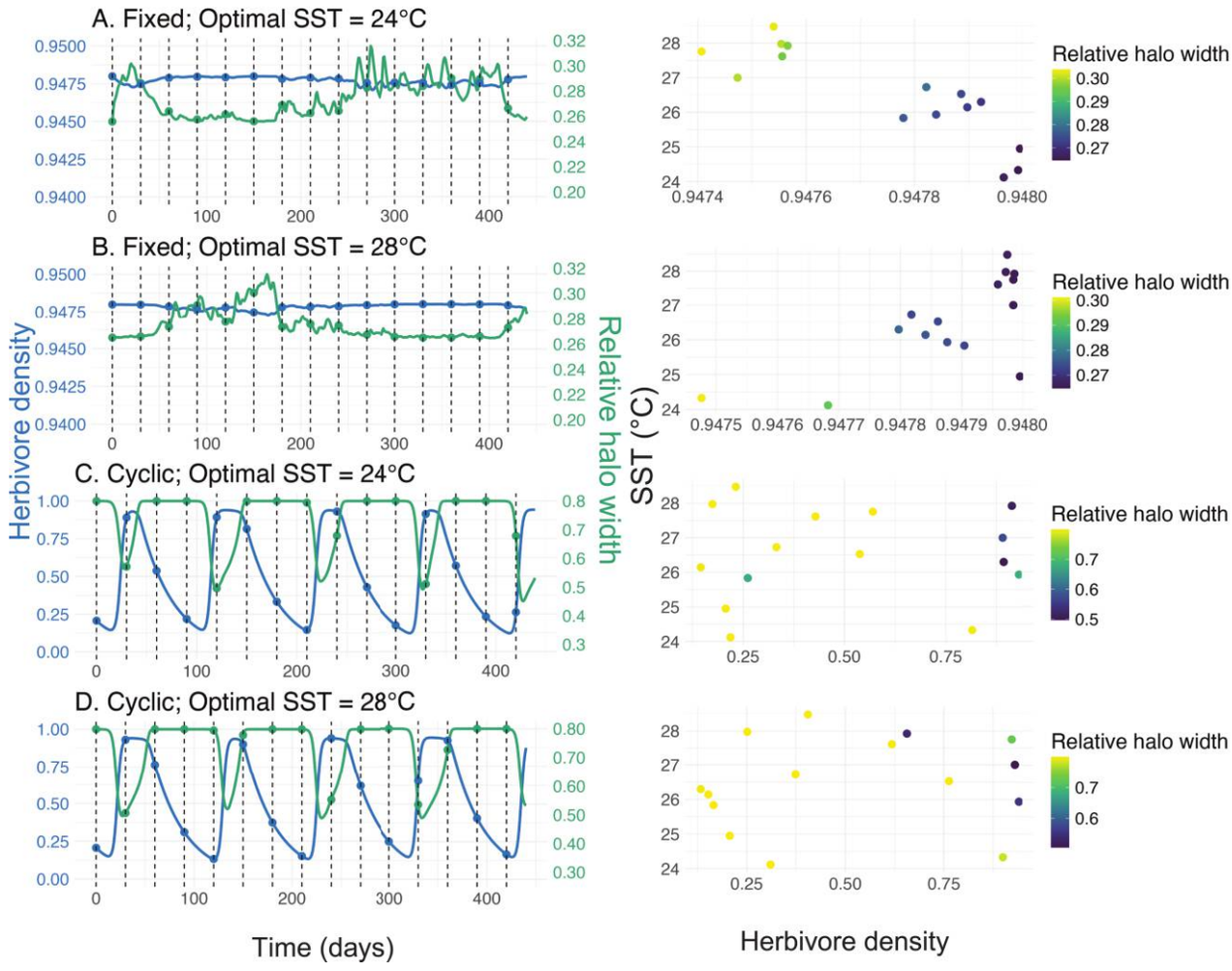

Figure 6: Simulations of sampling events occurring every 30 days (starting day 0) in our consumer-resource model. Parameters were $A_0 = 0.8, g = 2, k = 5, m = 0.03, r = 8, s = 6$, and $r_c = 2$. The left column shows the herbivore and halo width trajectories with dashed vertical lines every 30 days to represent sampling events. The right column shows how sea surface temperature (SST) and herbivore density affect halo width in these simulations. *A*, Fixed baseline model and optimal SST of 24°C. *B*, Fixed baseline model and optimal SST of 28°C. *C*, Cyclic baseline model and optimal SST of 24°C. *D*, Cyclic baseline model and optimal SST of 28°C.

support for the grazing hypothesis for halo formation and shed light on how temperature and primary productivity also contribute to halo dynamics. Some previous explanations of halos have been overly simplistic, given that there are complex underlying causes including foraging and nutrient cycling and not all halolike patterns may be created or maintained by the same mechanisms (Bilodeau et al. 2021). In the past, patch reef halos have been attributed to single explanations like herbivory (Randall 1965; Ogden et al. 1973; Hay 1984; Madin et al. 2011) or local hydrodynamics (Mitchell-Tapping 1975; Steiner and Willette 2014). More recently, it has become clear that a multitude of factors, both biotic and abiotic, have the potential to contribute to the formation and size fluctuation of halos (Madin et al. 2019*b*).

Biotic Factors

Grazing by herbivores is often considered to be the dominant direct mechanism behind the formation of reef halos (Ogden et al. 1973; Sweatman and Robertson 1994; Valentine and Heck 2005; Armitage and Fourqurean 2006; Valentine et al. 2007; Turgeon et al. 2010; Madin et al. 2011; Downie et al. 2013). Previous studies have demonstrated that predation risk is an indirect mechanism behind halo formation (e.g., Madin et al. 2010; Catano

et al. 2016), which follows that predation risk could indirectly create halos in natural reef settings as well as adjacent to artificial reefs (Einbinder et al. 2006). Madin et al. (2019*b*) used remote underwater video surveys to monitor fish and invertebrate grazing behavior on the reef adjacent to Heron Island, Australia, finding that herbivores and bioturbators rarely foraged as far as the halo boundary. In addition to predation risk, competition for resources may drive herbivores to make riskier decisions and graze further from the reef, as suggested by the fact that herbivore density also affects foraging distance (DiFiore et al. 2019; Madin et al. 2019*b*). Our findings support the hypothesis that herbivore grazing could mediate halo formation, given that our field study showed that higher herbivore biomass was correlated with halo presence and with lower halo vegetation density, while nonherbivore biomass was not. Interestingly, herbivore biomass did not correlate with halo width, which was linked only to temperature.

While behaviorally mediated factors (risk effects) are likely important to halo formation in general, we did not survey the large, roaming predator community. While we opportunistically observed predators such as the scalloped hammerhead and giant trevally near our sites and they have been documented in Kāneʻohe Bay (Bush and Holland 2002; Wetherbee et al. 2004), they are generally transient rather than residents. We surveyed only the resident fish community directly observed on our artificial reefs, which contained small piscivores such as snappers, but it is likely that additional unmeasured chronic predation risk on our reefs was generated by the occasional presence of wider-ranging predators. Some of the frequently observed herbivores were juvenile parrotfishes (not identified to species), which scrape microalgae (McAfee and Morgan 1996) and graze on seagrass (Kirsch et al. 2002; Maciá and Robinson 2005); surgeonfishes (ringtail surgeonfish *Acanthurus blocchi*, convict tang *Acanthurus triostegas*, yellow tang *Zebrasoma flavescens*), which feed on micro- and macroalgae (Tebbett et al. 2022); and damselfishes (Hawaiian sergeant *Abudefduf abdominalis*), which are generally planktivorous (Tyler 1992). Both parrotfishes and surgeonfishes have been found to alter their grazing patterns based on predation risk and contribute to halo formation in areas of seagrass as well as areas of macro- and microalgae (Sweatman and Robertson 1994; McAfee and Morgan 1996; Maciá and Robinson 2005). Coral reef fish in Hawaiʻi display site fidelity (Meyer et al. 2010), and juveniles in particular, which made up the majority of fish we surveyed, have small home ranges (Howard et al. 2013) and likely stayed as residents on our artificial reefs. Damselfishes are typically defined as residents, with limited movement and small home ranges, while parrotfishes and small surgeonfishes have been classified as semivagile species, meaning that their daily movements tend to fall within the tens of meters range (Friedlander and Parrish 1998). Herbivorous invertebrates (e.g., urchins) were not observed on our reefs.

We found that mean vegetation cover, a proxy for overall primary productivity, was the strongest predictor of halo vegetation density. Previous work found that the composition of background algae (analogous to our metric of mean vegetation cover) was a main predictor of halo presence and size (Madin et al. 2022). We were not able to distinguish vegetation types in our study, but future work could examine whether there is a successional effect of different vegetation types at the edges of the halo and offer insight into the relative importance of sediment disturbance versus direct consumption by specific grazers in creating and/or maintaining the halo. Besides grazing and primary productivity, spatially constrained bioturbation is another factor that can influence halo size (Madin et al. 2019*b*), which we did not account for in this study. There have been high rates of bioturbation and sedimentation measured in Kāneʻohe Bay (Smith and McMurtry 1995; Smith and Kukert 1996), so it is plausible that bioturbation played a role in the halo dynamics we observed.

Abiotic Factors

We also found evidence that temperature can contribute to halo dynamics. For example, temperature was a significant predictor of mean vegetation cover and halo width. We found that higher temperature led to less overall vegetation cover and larger halos. Previous work on the Great Barrier Reef associated SST with larger halos, although patch reef size was a confounding variable in this relationship (Madin et al. 2019*a*). For this reason, we chose to use artificially constructed reefs to ensure that reef size was consistent and to test potential hypothesized effects of temperature-dependent vegetation growth in our consumer-resource model. There are multiple possible reasons for the relationship we observed between halo size and temperature. There are strong seasonal dynamics in Kāneʻohe Bay with varied nutrient inputs (Drupp et al. 2011), which may correspond to vegetation species growing more in the cooler months of the year, when there are higher nutrient inputs because of rainfall, and leading to larger halos in the warmer summer months. It is also possible that herbivores are feeding more under higher temperatures as their metabolism increases (Volkoff and Rønnestad 2020), leading to larger halos.

However, we found that when there was high herbivore biomass, halos were more likely to be observed and were more distinct (less vegetation density inside the halo) at low temperatures than at high temperatures. Clearly, the interaction between temperature and herbivorous fish biomass affects multiple aspects of halo dynamics;

however, the exact mechanism of this interaction remains unclear. One possible explanation of this occurrence is that herbivore grazing behavior differs at different temperatures. This interaction could relate to herbivore preference for different vegetation species that dominate seasonally, leading to varied grazing behaviors and thus halo width. Grazing rates for tropical herbivorous fish, including parrotfishes and surgeonfishes, vary seasonally and were found to be highest in the summer in the Caribbean (Ferreira et al. 1998). These findings were due to fluctuations in temperature but also to other factors, such as food availability and seasonal differences in the nutrient content of algae (Ferreira et al. 1998). Although increased temperature likely increases grazing, warmer temperatures can also cause increased swimming behavior in fishes (Nilsson et al. 2019), which could cause both larger halos or the disappearance of a halo, if grazing is not concentrated near the reef. Cooler water can induce more lethargic behavior in fishes (Beitinger et al. 2000) and thus could increase fish grazing at close proximity to the reef. Future studies exploring the precise mechanism of how the spatial distribution of grazing changes across seasons could greatly benefit our understanding of halo presence and size fluctuation.

The relationship between temperature, fish community, and halo dynamics may vary across locations, depending on what conditions are optimal for both vegetation and the fish community. The amplitude of temperature and nutrient effects in our consumer-resource model varied widely depending on the optimal temperature or nutrient formulation used. The variation in results highlights that the scale of these effects may differ depending on the species in the system and their corresponding physiologies. We found that our simulated sampling data from the fixed model (representing a clustered scenario) with a low optimal temperature most closely resembled our in situ data, with relatively small-scale size fluctuations and where larger halos occurred with warmer temperature conditions. The cyclic dynamics observed in conditions with reduced vegetation growth (highly dispersed, low optimal temperature) somewhat reflect the larger-scale size fluctuations seen in natural halos (Madin et al. 2022; Ong et al. 2025). It is important to note that the parameter values used in the consumer-resource model are mostly arbitrary and, aside from the reef-clustering (R) scenarios, do not necessarily represent our Kāneʻohe Bay sites. We conducted this analysis to investigate the potential qualitative outcomes, such as fixed or cyclic halos. Overall, our goal with this comparison was to determine where our field data aligned within the spectrum of theoretical predictions. We did not include temperature-dependent fish consumption (e.g., increasing metabolic demand with higher SST) in our consumer-resource model, but future studies could incorporate it as another mechanism by which temperature could drive halo system dynamics and shed further light on the complex interactions we observed in our field study.

Nutrients may be an important driver of systems with halos, but their effect on halo dynamics remains unclear. While the nutrients we measured did not correlate with mean vegetation cover, we were able to take only monthly measurements. It would have been preferable to obtain a more continuous time series of nutrients, as we did for temperature. Nutrient concentrations in Kāneʻohe Bay can fluctuate rapidly (Ringuet and Mackenzie 2005) and thus could produce different values from day to day. The uncertainty around nutrient effects on halos may also be due to the multiple interactive ways by which nutrients can affect system dynamics. In the absence of other factors, increased nutrients should increase primary productivity, and thus vegetation density, near reefs. However, previous studies have found a counterintuitive pattern where heightened nutrients corresponded to larger halos (Alevizon 2002). A possible explanation for this finding is that the nutrient availability might increase epibiont growth and thus increase herbivore consumption of vegetation, given that epibionts are the preferred food of many grazers (Alevizon 2002; Campbell et al. 2018; Goss et al. 2018). Another way that nutrients could affect halo dynamics is by increasing the nutrient content of reef-adjacent vegetation and therefore increasing its consumption by grazers (Campbell et al. 2018). Additionally, fish-derived nutrients play an important role in shaping marine vegetation through their impact on productivity. Fish can increase nutrient availability surrounding the structures where they aggregate, which could increase growth of adjacent vegetation (Allgeier et al. 2013; Layman et al. 2013). Essentially, increased nutrients could increase or decrease local vegetation cover depending on herbivore responses and changes in productivity rates (Bilodeau et al. 2021); these interactions may explain the difficulty in isolating their exact effects on halo dynamics.

We found that temperature and nutrient impacts can manifest differently at different scales and/or spatial clustering of reefs through our consumer-resource model. Essentially, the temperature and nutrient formulations had larger effects on a clustered reef system with fixed baseline dynamics, where there may be more movement of herbivores and less consistent grazing pressure. When the system was already fluctuating, such as in the dispersed scenario, the effects of adding temperature and nutrient dependencies were generally smaller. Future work could involve a spatially explicit model of reef halo dynamics to more fully capture how halo width and distinctness change with varied predation risk and environmental variables.

Other abiotic factors, such as wave action, could also be a cause of halo patterns, as was found in the US Virgin

Islands and Dominica (Mitchell-Tapping 1975; Steiner and Willette 2014). In other cases, however, hydrodynamics were not found to result in halos, especially for cases in shallow lagoon environments with minimal current and reduced waves (Randall 1965; Bilodeau et al. 2021). Kāneʻohe Bay is an enclosed and well-protected area; its physical properties are controlled by precipitation, stream runoff, and evaporation with minimal effects of waves and tides (Drupp et al. 2011). The sandbar where the artificial reefs were located is a shallow, protected area; thus, we would not expect significant hydrodynamics effects, which is demonstrated in part by the fact that our small artificial reefs remained in position for 2 years without any attachment to the substrate. However, we did not test the role of hydrodynamics in this study.

Conclusion

To use halo patterns to make inferences on coral reef and reef fish health, we must have a full understanding of the suite of mechanisms that can create halos and cause halo size fluctuations. Here, we have provided further evidence that there are a multitude of both biotic and abiotic factors that each play a role in shaping vegetation patterns surrounding reefs. Our results suggest that factors such as overall primary productivity, SST, and herbivore biomass can mediate halo presence and size fluctuations. By exploring this question with both an in situ field study and a mechanistic consumer-resource model, our results provide insight into both correlative and potential causal effects of certain biotic and abiotic drivers on halo dynamics. These findings bring us closer to uncovering the full suite of mechanisms at play in the creation and maintenance of the intriguing global phenomenon of reef halos.

Acknowledgments

We thank Megan Donahue, Tye Kindinger, and Amelia Meier for analysis advice; Aviv Suan for field logistics help; Danielle Hull and University of Hawaiʻi SOEST Lab for Analytical Biogeochemistry for conducting nutrient analysis; and everyone who volunteered their time to assist in the field: Mollie Asbury, Ray Crichton, Nathan Fitzpatrick, Simone Franceschini, Kevin Frey, Natalie Goeler-Slough, Aʻaliʻi Kelling, Zack Rago, Jacob Snyder, Eleanor Sterling, Alyssa Veneri, and Shreya Yadav. We also thank the reviewers and editors for their constructive comments.

Statement of Authorship

A.A.I.-G. was responsible for conceptualization, funding acquisition, methods development/experimental design, data collection, data analysis, data visualization, supervision, and writing the original draft. E.M.P.M. and L.C.M. were responsible for conceptualization, funding acquisition, methods development/experimental design, supervision, and reviewing and editing the manuscript. E.L. and T.W.O. were responsible for data analysis and reviewing and editing the manuscript. A.C.M., S.A.R., J.B.P., A.T., and D.W. were responsible for data collection and reviewing and editing the manuscript.

Data and Code Availability

All data and code are available at GitHub (https://github.com/ainnesgold/kbay_halos_2025) and archived at Zenodo (https://doi.org/10.5281/zenodo.15640306; Innes-Gold 2025)

Literature Cited

Akoglu, H. 2018. User's guide to correlation coefficients. Turkish Journal of Emergency Medicine 18:91–93. https://doi.org/10.1016/j.tjem.2018.08.001.

Alevizon, W. 2002. Enhanced seagrass growth and fish aggregations around Bahamian patch reefs: the case for a functional connection. Bulletin of Marine Science 70:957–966.

Alevizon, W. S., and J. C. Gorham. 1989. Effects of artificial reef deployment on nearby resident fishes. Bulletin of Marine Science 44:646–661.

Allgeier, J. E., L. A. Yeager, and C. A. Layman. 2013. Consumers regulate nutrient limitation regimes and primary production in seagrass ecosystems. Ecology 94:521–529.

Almany, G. R. 2004. Differential effects of habitat complexity, predators and competitors on abundance of juvenile and adult coral reef fishes. Oecologia 141:105–113.

Armitage, A. R., and J. W. Fourqurean. 2006. The short-term influence of herbivory near patch reefs varies between seagrass species. Journal of Experimental Marine Biology and Ecology 339:65–74.

Baddeley, A., E. Rubak, and R. Turner. 2015. Spatial point patterns: methodology and applications with R. CRC, Boca Raton, FL.

Bates, D., M. Mächler, B. Bolker, and S. Walker. 2015. Fitting linear mixed-effects models using lme4. Journal of Statistical Software 67:1–48.

Beitinger, T. L., W. A. Bennett, and R. W. McCauley. 2000. Temperature tolerances of North American freshwater fishes exposed to dynamic changes in temperature. Environmental Biology of Fishes 58:237–275.

Bilodeau, S. M., C. A. Layman, and M. R. Silman. 2021. Benthic pattern formation in shallow tropical reefscapes: does grazing explain grazing halos? Landscape Ecology 36:1605–1620.

Bristow, L. A., W. Mohr, S. Ahmerkamp, and M. M. M. Kuypers. 2017. Nutrients that limit growth in the ocean. Current Biology 27:R474–R478.

Bush, A., and K. Holland. 2002. Food limitation in a nursery area: estimates of daily ration in juvenile scalloped hammerheads, *Sphyrna lewini* (Griffith and Smith, 1834) in Kane'ohe Bay, O'ahu, Hawai'i. Journal of Experimental Marine Biology and Ecology 278:157–178.

Campbell, J. E., A. H. Altieri, L. N. Johnston, C. D. Kuempel, R. Paperno, V. J. Paul, and J. E. Duffy. 2018. Herbivore community

determines the magnitude and mechanism of nutrient effects on subtropical and tropical seagrasses. Journal of Ecology 106:401–412.

Catano, L. B., M. C. Rojas, R. J. Malossi, J. R. Peters, M. R. Heithaus, J. W. Fourqurean, and D. E. Burkepile. 2016. Reefscapes of fear: predation risk and reef heterogeneity interact to shape herbivore foraging behaviour. Journal of Animal Ecology 85:146–156.

Clark, P. J., and F. C. Evans. 1954. Distance to nearest neighbor as a measure of spatial relationships in populations. Ecology 35:445–453.

Clark, S., and A. J. Edwards. 1994. Use of artificial reef structures to rehabilitate reef flats degraded by coral mining in the Maldives. Bulletin of Marine Science 55:724–744.

Collier, C. J., Y. X. Ow, L. Langlois, S. Uthicke, C. L. Johansson, K. R. O'Brien, V. Hrebien, and M. P. Adams. 2017. Optimum temperatures for net primary productivity of three tropical seagrass species. Frontiers in Plant Science 8:1446. https://doi.org/10.3389/fpls.2017.01446.

Cott, G. M., J. S. Caplan, and T. J. Mozdzer. 2018. Nitrogen uptake kinetics and saltmarsh plant responses to global change. Scientific Reports 8:5393.

Dailer, M. L., J. E. Smith, and C. M. Smith. 2012. Responses of bloom forming and non-bloom forming macroalgae to nutrient enrichment in Hawai'i, USA. Harmful Algae 17:111–125.

DiFiore, B. P., S. A. Queenborough, E. M. P. Madin, V. J. Paul, M. B. Decker, and A. C. Stier. 2019. Grazing halos on coral reefs: predation risk, herbivore density, and habitat size influence grazing patterns that are visible from space. Marine Ecology Progress Series 627:71–81.

Downie, R., R. Babcock, D. Thomson, and M. Vanderklift. 2013. Density of herbivorous fish and intensity of herbivory are influenced by proximity to coral reefs. Marine Ecology Progress Series 482:217–225.

Drupp, P., E. H. De Carlo, F. T. Mackenzie, P. Bienfang, and C. L. Sabine. 2011. Nutrient inputs, phytoplankton response, and CO_2 variations in a semi-enclosed subtropical embayment, Kaneohe Bay, Hawaii. Aquatic Geochemistry 17:473–498.

Einbinder, S., A. Perelberg, O. Ben-Shaprut, M. H. Foucart, and N. Shashar. 2006. Effects of artificial reefs on fish grazing in their vicinity: evidence from algae presentation experiments. Marine Environmental Research 61:110–119.

Ferguson, A. M., E. S. Harvey, M. D. Taylor, and N. A. Knott. 2013. A herbivore knows its patch: Luderick, *Girella tricuspidata*, exhibit strong site fidelity on shallow subtidal reefs in a temperate marine park. PLoS ONE 8:e65838.

Ferreira, D. E. L., A. C. Peret, and R. Coutinho. 1998. Seasonal grazing rates and food processing by tropical herbivorous fishes. Journal of Fish Biology 53:222–235.

Friedlander, A. M., and J. D. Parrish. 1998. Habitat characteristics affecting fish assemblages on a Hawaiian coral reef. Journal of Experimental Marine Biology and Ecology 224:1–30.

Froese, R., and D. Pauly. 2024. FishBase. https://www.fishbase.org.

Garrett, P., D. L. Smith, A. O. Wilson, and D. Patriquin. 1971. Physiography, ecology, and sediments of two Bermuda patch reefs. Journal of Geology 79:647–668.

Goss, H., J. Jaskiel, and R. Rotjan. 2018. *Thalassia testudinum* as a potential vector for incorporating microplastics into benthic marine food webs. Marine Pollution Bulletin 135:1085–1089.

Hay, M. E. 1984. Patterns of fish and urchin grazing on Caribbean coral reefs: are previous results typical? Ecology 65:446–454.

Hillman, K., A. J. McComb, and D. I. Walker. 1995. The distribution, biomass and primary production of the seagrass *Halophila ovalis* in the Swan/Canning Estuary, Western Australia. Aquatic Botany 51:1–54.

Howard, K. G., J. T. Claisse, T. B. Clark, K. Boyle, and J. D. Parrish. 2013. Home range and movement patterns of the redlip parrotfish (*Scarus rubroviolaceus*) in Hawaii. Marine Biology 160:1583–1595.

Ingestad, T. 1976. Nitrogen and cation nutrition of three ecologically different plant species. Physiologia Plantarum 38:29–34.

Innes-Gold, A. 2025. Data from: Herbivory and temperature mediate coral reef halo dynamics. American Naturalist, Zenodo, https://doi.org/10.5281/zenodo.15640307.

Kirsch, K., J. Valentine, and K. Heck. 2002. Parrotfish grazing on turtlegrass *Thalassia testudinum*: evidence for the importance of seagrass consumption in food web dynamics of the Florida Keys National Marine Sanctuary. Marine Ecology Progress Series 227:71–85.

Layman, C. A., J. E. Allgeier, L. A. Yeager, and E. W. Stoner. 2013. Thresholds of ecosystem response to nutrient enrichment from fish aggregations. Ecology 94:530–536.

Lee, K.-S., S. R. Park, and Y. K. Kim. 2007. Effects of irradiance, temperature, and nutrients on growth dynamics of seagrasses: a review. Journal of Experimental Marine Biology and Ecology 350:144–175.

Maciá, S., and M. P. Robinson. 2005. Effects of habitat heterogeneity in seagrass beds on grazing patterns of parrotfishes. Marine Ecology Progress Series 303:113–121.

Madin, E. M. P., S. D. Gaines, J. S. Madin, and R. R. Warner. 2010. Fishing indirectly structures macroalgal assemblages by altering herbivore behavior. American Naturalist 176:785–801.

Madin, E. M. P., A. R. Harborne, A. M. T. Harmer, O. J. Luiz, T. B. Atwood, B. J. Sullivan, and J. S. Madin. 2019*a*. Marine reserves shape seascapes on scales visible from space. Proceedings of the Royal Society B 286:20190053.

Madin, E. M. P., J. S. Madin, and D. J. Booth. 2011. Landscape of fear visible from space. Scientific Reports 1:14.

Madin, E. M. P., K. Precoda, A. R. Harborne, T. B. Atwood, C. M. Roelfsema, and O. J. Luiz. 2019*b*. Multi-trophic species interactions shape seascape-scale coral reef vegetation patterns. Frontiers in Ecology and Evolution 7:102.

Madin, E. M. P., K. Precoda, C. M. Roelfsema, and A. Suan. 2022. Global conservation potential in coral reef halos: consistency over space, time, and ecosystems worldwide. American Naturalist 200:857–871.

McAfee, S. T., and S. G. Morgan. 1996. Resource use by five sympatric parrotfishes in the San Blas Archipelago, Panama. Marine Biology 125:427–437.

Meyer, C. G., Y. P. Papastamatiou, and T. B. Clark. 2010. Differential movement patterns and site fidelity among trophic groups of reef fishes in a Hawaiian marine protected area. Marine Biology 157:1499–1511.

Mitchell-Tapping, H. J. 1975. Wave effect on sea grasses in the West Indies: the formation of the bare sand zone. Geological Magazine 112:515–518.

Monfet, E., and A. Unc. 2017. Defining wastewaters used for cultivation of algae. Algal Research 24:520–526.

Nilsson, J., L. Moltumyr, A. Madaro, T. S. Kristiansen, S. K. Gåsnes, C. M. Mejdell, K. Gismervik, et al. 2019. Sudden exposure to warm water causes instant behavioural responses indicative of nociception or pain in Atlantic salmon. Veterinary and Animal Science 8:100076.

Ogden, J. C., R. A. Brown, and N. Salesky. 1973. Grazing by the echinoid *Diadema antillarum* Philippi: formation of halos around West Indian patch reefs. Science 182:715–717.

Ong, T. W., L. C. McManus, V. V. Vasconcelos, L. Yang, and C. Su. 2025. Seeing halos: spatial and consumer-resource constraints to landscapes of fear. American Naturalist 205:590–603.

Ralph, P. 1998. Photosynthetic response of laboratory-cultured *Halophila ovalis* to thermal stress. Marine Ecology Progress Series 171:123–130.

Randall, J. E. 1965. Grazing effect on sea grasses by herbivorous reef fishes in the West Indies. Ecology 46:255–260.

R Core Team. 2024. R: a language and environment for statistical computing. R Foundation for Statistical Computing, Vienna.

Rier, S. T., and R. J. Stevenson. 2006. Response of periphytic algae to gradients in nitrogen and phosphorus in streamside mesocosms. Hydrobiologia 561:131–147.

Ringuet, S., and F. Mackenzie. 2005. Controls on nutrient and phytoplankton dynamics during normal flow and storm runoff conditions, southern Kaneohe Bay, Hawaii. Estuaries 28:327–337.

Schneider, C. A., W. S. Rasband, and K. W. Eliceiri. 2012. NIH Image to ImageJ: 25 years of image analysis. Nature Methods 9:671–675.

Singh, S. P., and P. Singh. 2015. Effect of temperature and light on the growth of algae species: a review. Renewable and Sustainable Energy Reviews 50:431–444.

Smith, C. R., and K. Kukert. 1996. Macrobenthic community structure, secondary production, and rates of bioturbation and sedimentation at the Kane'ohe Bay lagoon floor. Pacific Science 50:211–229.

Smith, C. R., and G. M. McMurtry. 1995. Rates of sedimentation in Kaneohe Bay lagoon based on Pb-210 geochronology and Cs-137 penetration depths. Final Report to State of Hawaii. Department of Land and Natural Resources, Honolulu.

Steiner, S. C. C., and D. A. Willette. 2014. Dimming sand halos around coral reefs in Dominica: new expansion corridors for the invasive seagrass *Halophila stipulacea*. ITME Research Reports 32B:1–3.

Sweatman, H., and D. R. Robertson. 1994. Grazing halos and predation on juvenile Caribbean surgeonfishes. Marine Ecology Progress Series 111:1–6.

Tebbett, S. B., A. C. Siqueira, and D. R. Bellwood. 2022. The functional roles of surgeonfishes on coral reefs: past, present and future. Reviews in Fish Biology and Fisheries 32:387–439.

Turgeon, K., A. Robillard, J. Grégoire, V. Duclos, and D. L. Kramer. 2010. Functional connectivity from a reef fish perspective: behavioral tactics for moving in a fragmented landscape. Ecology 91:3332–3342.

Tyler, W. A. 1992. The spatial and temporal dynamics of colonial nesting in the maomao, *Abudefduf abdominalis* (Family: Pomacentridae). PhD diss. University of Hawai'i, Mānoa.

Valentine, J. F., and K. L. Heck. 2005. Perspective review of the impacts of overfishing on coral reef food web linkages. Coral Reefs 24:209–213.

Valentine, J., J. K. L. Heck, D. Blackmon, M. Goecker, J. Christian, R. Kroutil, K. Kirsch, et al. 2007. Food web interactions along seagrass coral reef boundaries: effects of piscivore reductions on cross-habitat energy exchange. Marine Ecology Progress Series 333:37–50.

Volkoff, H., and I. Rønnestad. 2020. Effects of temperature on feeding and digestive processes in fish. Temperature 7:307–320.

Welsh, J. Q., and D. R. Bellwood. 2012. How far do schools of roving herbivores rove? a case study using *Scarus rivulatus*. Coral Reefs 31:991–1003.

Wetherbee, B. M., K. N. Holland, C. G. Meyer, and C. G. Lowe. 2004. Use of a marine reserve in Kaneohe Bay, Hawaii by the giant trevally, *Caranx ignobilis*. Fisheries Research 67:253–263.

Wood, S. N. 2017. Generalized additive models: an introduction with R. 2nd ed. CRC, Boca Raton, FL.

References Cited Only in the Online Enhancements

Armstrong, F. A. J., C. R. Stearns, and J. D. H. Strickland. 1967. The measurement of upwelling and subsequent biological process by means of the Technicon Autoanalyzer and associated equipment. Deep Sea Research and Oceanographic Abstracts 14:381–389.

Grasshoff, K., K. Kremling, and M. Ehrhardt. 2009. Methods of seawater analysis. Wiley, Weinheim, Germany.

Murphy, J., and J. P. Riley. 1962. A modified single solution method for the determination of phosphate in natural waters. Analytica Chimica Acta 27:31–36.

Associate Editor: Egbert H. van Nes
Editor: Erol Akçay

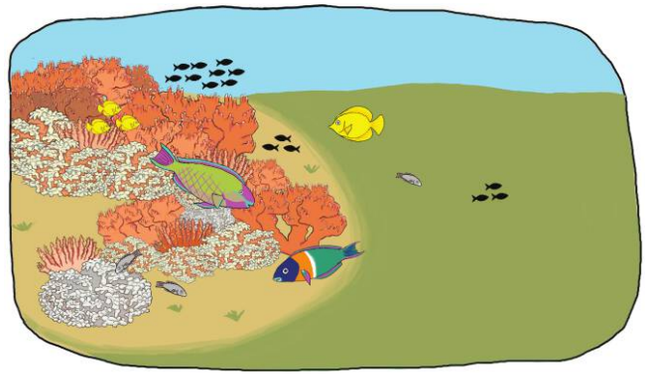

Graphic representation of a reef halo. Artist: Anne A. Innes-Gold.